Observation of coherence transfer by electron-electron correlation

R. Grobe and J. H. Eberly
Department of Physics and Astronomy, University of Rochester, Rochester, New York 14627
(Received 14 December 1992)

We present the results of exact wave-function calculations that are equivalent to numerical experiments on a two-electron quantum system. We show that Rabi oscillations of the core electron can modify the photoelectron spectrum of the outer electron by efficient coherence transfer via *e-e* correlation, even in the absence of an autoionizing level or other continuum structure. We compare a simplified analytically soluble two-electron theory with our numerical results.

PACS number(s): 32.80.Rm, 32.80.Fb, 32.80.Wr

In the present paper we introduce a two-electron coherence process that is similar to the one-electron Autler-Townes effect [1]. This process exhibits unexpected features that are not found in the one-electron effect. In the photoelectron spectrum we find a new doublet in addition to the one predicted by Knight [2,3]. There is a novel dressed-state reversal, i.e., the *higher*-energy peak in the new doublet comes from the *lower*-energy dressed bound state. In addition, the ground- (initial) state probability decays *without* Rabi oscillations confirming that there is *no autoionizing state participating in this effect.*

This coherence process was first observed in numerical experiments carried out on a two-electron "atom" that is the one-dimensional analog of a negative ion in a laser field. Fully correlated two-electron wave functions were calculated for this atom and analyzed to obtain various time-dependent and energy-dependent probabilities, which we will present below. Our artificial two-electron atom has been discussed before [4,5], and its bare Hamiltonian is given by

$$H_0=\tfrac{1}{2}p_1^2+\tfrac{1}{2}p_2^2+V(x_1)+V(x_2)-V(x_1-x_2)\ . \quad (1)$$

Here x_1 and x_2 are the coordinates of electrons 1 and 2, and the soft-core Coulombic potential $V(x)=-1/(x^2+1)^{1/2}$ governs both the attractive electron-proton and the repulsive electron-electron interactions. This one-proton–two-electron system shares many features with real negative ions. For example, it has only one bound state. The core-electron binding energy is approximately equal to 11 times the outer electron's detachment energy, just as in all alkali-metal negative ions, Li^-, Na^-, K^-, etc. The one-electron detachment thresholds are available [5] and the one-electron core system has been used repeatedly for studies of atomic systems in a strong laser field [6].

The interaction of this system with a laser field is determined by the time-dependent Schrödinger equation (in dimensionless atomic units)

$$i\frac{\partial\Psi(x_1,x_2,t)}{\partial t}=[H_0+(x_1+x_2)E(t)]\Psi(x_1,x_2,t)\ , \quad (2)$$

where the laser field is $E(t)=\mathcal{E}(t)\sin\omega_L t$, the pulse shape is given by the smooth function $\mathcal{E}(t)=\mathcal{E}_0\sin^2(\pi t/T)$, and ω_L is the laser frequency. We have prepared the electrons initially in the ground state (which is automatically symmetric under electron coordinate exchange). Solutions of the time-independent and time-dependent Schrödinger equations are accomplished numerically on a spatial grid by methods that have been described before [7].

For later reference we have sketched in Fig. 1 the low-lying bare energy levels for our negative ion, showing schematically what we believe to be a useful indication of the dynamics leading to our experimental data. On the left side we show the energy levels that we associate with the weakly bound outer electron (photodetachment potential of 0.06 a.u.) and on the right side we show the lowest several discrete levels of the core electron. In Fig. 2 we give an alternative view of the level scheme that is based on two-electron energies. The ground state is the

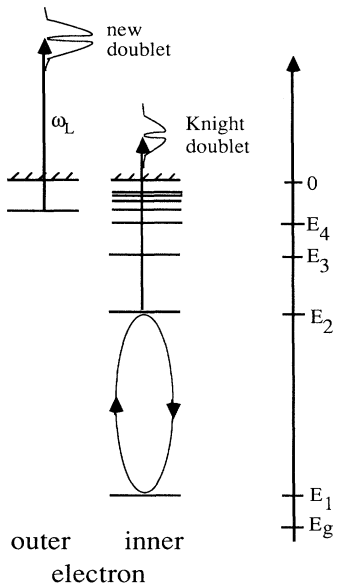

FIG. 1. An energy-level diagram for the negative-ion model based on an independent-electron picture for the weakly bound "outer" and strongly bound "inner" electron.

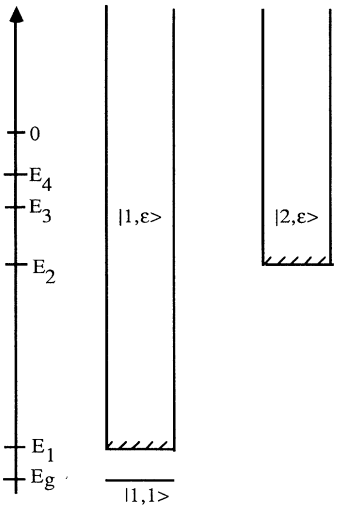

FIG. 2. Total-energy diagram, but only the ground state at $E_g=-0.73$ a.u. and the first two continua beginning at $E_1=-0.67$ a.u. and $E_2=-0.275$ a.u. have been displayed.

only bound state. The continua above the first and second thresholds are associated with the core-electron ground state at $E_1=-0.670$ a.u. and first core excited state at $E_2=-0.275$ a.u. In both Figs. 1 and 2 we have drawn the same vertical energy scale.

Our procedure is to solve Schrödinger's equation for $\Psi(x_1,x_2,t)$ and then analyze it after a smooth laser turnoff at time $t=T$. We can obtain the photoelectron energy spectra $P(\varepsilon)$ and all of the low-lying bound-state probabilities by appropriate projections [5]. In almost all of the experiments described here we limited the laser field strength to $\mathcal{E}_0=0.05$ a.u. (laser intensity slightly less than 10^{14} W/cm^2), and scanned the frequency of the incident laser. The most interesting frequencies are in the neighborhood of the core electron's $n=1$ to $n=2$ resonance.

The resonant Rabi cycling indicated in Fig. 1 for the core electron suggests [2] that a doublet should be found in the core electron's photospectrum with energy ω_L above the $n=2$ state, i.e., with kinetic energy given by $\varepsilon=\omega_L+E_2\approx(E_2-E_1)+E_2=0.395+(-0.275)\approx0.120$ a.u., and this is indeed the case. The splitting of the peaks should be equal to the resonant Rabi frequency and this is also the case [8]. Thus the familiar one-electron Autler-Townes effect (and so-called Knight photoelectron doublet) is present. However, a new and much stronger doublet is found centered at a different higher energy $\varepsilon\approx0.335$ a.u. These two photoelectron doublets are shown in Fig. 3. The stronger and higher doublet has apparently not been predicted previously.

We have carried out a series of wave-function calculations to study the higher doublet. For a variety of values of the laser frequency ω_L we calculated the photoelectron spectrum as well as the time dependence of various level populations. In Fig. 4, we show three photoelectron spectra. The typical case (a) or (c) finds a single photopeak, and its energy can be seen to be $\varepsilon\approx\omega_L-0.06$ a.u. Since 0.06 a.u. is the binding energy of the *outer* electron

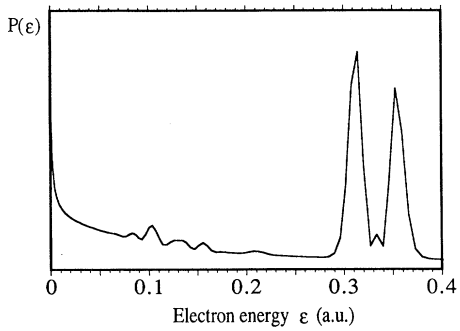

FIG. 3. Photoelectron spectral structure created by a sine-squared incident laser pulse with $\mathcal{E}_0=0.05$ a.u., $\omega_L=0.395$ a.u., and $T=40$ cycles. Details near to the higher split peak are shown again in Fig. 4(b).

it is compelling to conclude that this is simply the normal photopeak associated with detachment of the outer electron. The exceptional case is the double peak in (b). The question is how to understand both its location and its splitting since the outer electron has no bound-bound resonances at all (and the system's autodetaching resonances are not in the spectral region involved here).

We interpret the peak splitting common to Figs. 3 and 4(b) as arising from two-electron coherence transfer from the core electron to the outer electron when the core elec-

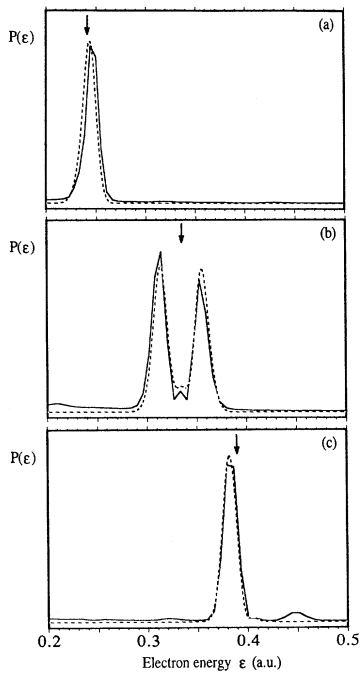

FIG. 4. Three photoelectron spectra. The arrow indicates the kinetic energy predicted for outer-electron photodetachment: $\varepsilon=-0.06$ a.u. $+\omega_L$. The dashed curves are predictions of Eqs. (6). The incident laser frequencies are (a) $\omega_L=0.30$ a.u.; (b) $\omega_L=0.395$ a.u. $\approx E_{21}$; and (c) $\omega_L=0.45$ a.u. Note that Fig. 4(b) is identical with the upper part of Fig. 3.

tron is resonantly excited. We can picture the transfer mechanism as arising from the periodic change of the outer electron's binding potential due to the Rabi oscillations of the core electron. Or we can say that the core electron's resonant transitions periodically change the type of continuum which characterizes the photodetachment state. In any event it is remarkable that the coherence transfer is as strong as it is.

We have found that a relatively simple theoretical model can be developed to support our interpretation of two-electron coherence transfer. Our model can be solved analytically and could be applied to any two-electron system. It accounts for the spectral phenomena of Fig. 4 as well as associated temporal phenomena. We now describe this model.

First in Fig. 5 we repeat Fig. 2, with two one-photon transitions shown. In this way we indicate in Fig. 5 the subspace of relevant eigenstates of the bare two-electron Hamiltonian. These are states that are strongly connected to the ground state, which serves as our two-electron initial state. To simplify our notation we will use state labels based on the independent-particle picture of Fig. 1(a). We denote the ground state by $|1,1\rangle$. In addition there are the two mutually orthogonal continuum states $|1,\varepsilon\rangle$ and $|2,\varepsilon\rangle$, which describe a free outer electron with energy ε and a core electron in its ground state or first excited state. We neglect other states, which are dynamically not so important, and write the time-dependent system wave function as

$$|\Psi(t)\rangle = G(t)|1,1\rangle + \int d\varepsilon\, B(\varepsilon,t)|1,\varepsilon\rangle + \int d\varepsilon\, C(\varepsilon,t)|2,\varepsilon\rangle \ . \tag{3}$$

The time evolution of these states is governed by an effective two-electron Hamiltonian

$$H_{\text{eff}}(t) = E_g|1,1\rangle\langle 1,1| + \int d\varepsilon (E_1+\varepsilon)|1,\varepsilon\rangle\langle 1,\varepsilon| + \int d\varepsilon (E_2+\varepsilon)|2,\varepsilon\rangle\langle 2,\varepsilon| + \int d\varepsilon\, g(\varepsilon,t)\{|1,1\rangle\langle 1,\varepsilon| + |1,\varepsilon\rangle\langle 1,1|\} + \int d\varepsilon \int d\varepsilon' \Omega(\varepsilon,\varepsilon',t)\{|1,\varepsilon\rangle\langle 2,\varepsilon'| + |2,\varepsilon'\rangle\langle 1,\varepsilon|\} \ , \tag{4}$$

which couples the ground state $|1,1\rangle$ to the first continuum $|1,\varepsilon\rangle$ (an outer-electron transition) and which allows for a core transition of the inner electron from state $|1,\varepsilon\rangle$ to $|2,\varepsilon'\rangle$. The dipole moment coupling strengths are given by

$$g(\varepsilon,t) \equiv E(t)\langle 1,1|(x_1+x_2)|1,\varepsilon\rangle \equiv E(t)g(\varepsilon) \ ,$$

$$\Omega(\varepsilon,\varepsilon',t) \equiv E(t)\langle 1,\varepsilon|(x_1+x_2)|2,\varepsilon'\rangle \tag{5a}$$

$$\approx E(t)\langle 1|x|2\rangle \delta(\varepsilon-\varepsilon') \equiv \Omega_0(t)\delta(\varepsilon-\varepsilon') \ . \tag{5b}$$

The coupling $\Omega(\varepsilon,\varepsilon',t)$ can be calculated by approximating the states $|1,\varepsilon\rangle$ and $|2,\varepsilon'\rangle$ by the product of the corresponding monoelectronic states. The effective Hamiltonian (4) generates the following equations of motion for the state amplitudes:

$$i\frac{\partial G(t)}{\partial t} = E_g G(t) + \int d\varepsilon\, g(\varepsilon,t)B(\varepsilon,t) \ , \tag{6a}$$

$$i\frac{\partial B(\varepsilon,t)}{\partial t} = (E_1+\varepsilon)B(\varepsilon,t) + \Omega_0(t)C(\varepsilon,t) + g(\varepsilon,t)G(t) \ , \tag{6b}$$

$$i\frac{\partial C(\varepsilon,t)}{\partial t} = (E_2+\varepsilon)C(\varepsilon,t) + \Omega_0(t)B(\varepsilon,t) \ . \tag{6c}$$

By making the usual assumptions about the flatness of the continuum [$g(\varepsilon)\approx$const] and the rotating-wave approximation, we can find an analytical solution for Eqs. (6), for example by using Laplace transforms. If we additionally assume a square laser pulse $\mathcal{E}(t)=\mathcal{E}_0$ we can obtain a closed-form expression for the photoelectron energy spectrum in the first continuum:

$$|B(\varepsilon,t)|^2 = c\left|\frac{\Omega_0^2}{2\Omega(\Omega+\Delta)}\frac{\exp(-\gamma t)-\exp(-i\mu_+ t)}{\mu_+ + i\gamma} + \frac{\Omega_0^2}{2\Omega(\Omega-\Delta)}\frac{\exp(-\gamma t)-\exp(-i\mu_- t)}{\mu_- + i\gamma}\right|^2 . \tag{7}$$

Here $\Delta=(E_2-E_1-\omega_L)$ denotes the detuning of the two discrete core levels, $\gamma=\pi g^2$ denotes the ground-state amplitude decay rate, $\Omega=(\Delta^2+\Omega_0^2)^{1/2}$ is the (generalized)

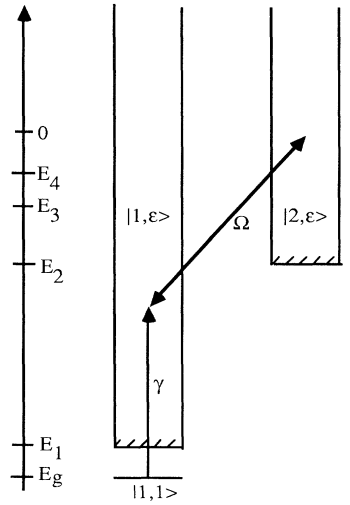

FIG. 5. Same energy-level diagram as in Fig. 2. The two one-photon transitions and the corresponding dipole couplings as defined in the analytically soluble model are shown.

Rabi frequency, $\Omega_0=\mathcal{E}_0\langle 1|x|2\rangle$ is the Rabi frequency, $\mu_\pm=\Delta_\varepsilon+\Delta/2\pm\Omega/2$ are the two (dressed) Floquet frequencies, $\Delta\varepsilon=-E_g+E_1+\varepsilon-\omega_L$ is the detuning from the ground state, and C is a normalization factor. A possible laser-induced ground-state shift would correspond to an imaginary part of γ which is not necessary here.

The notation used in (7) makes it apparent that the solution has a dressed-state interpretation. This dressed-state interpretation has some unusual features. For large positive detuning $\Delta\gg\Omega_0$ the second term corresponds to the *upper* (elastic) photoelectron peak (with energy $\varepsilon=E_g-E_1+\omega_L+\Omega_0^2/4\Delta$), which has to be associated with the *lower* of the two dressed states. The *lower*-lying (inelastic) peak at $\varepsilon=E_g-E_1+\omega_L-\Delta-\Omega_0^2/4\Delta$ thus corresponds to the *upper* dressed state with quasienergy μ_+ described by the first term. This correspondence between photopeaks and dressed states is exactly opposite to the case of one-photon-resonant two-photon ionization [2]. The special case of a forbidden core transition ($\Omega_0=0$) is also contained in formula (7). The inelastic amplitude vanishes in this limit and we find the well-known Lorentzian shaped single photopeak in the long-time limit.

Formula (7) correctly predicts these features: the existence of a singlet or doublet photopeak depending on Δ, the positions and relative heights and widths of the peaks, peak splitting proportional to $\mathcal{E}_0$, etc. A real experimental situation, however, would not involve a square laser pulse so we have also solved Eqs. (6) for a smooth time-dependent sine-squared pulse with the same laser parameters that were used in the original computer experiments. The resulting predictions for photoelectron spectra are shown as the dotted lines in Fig. 4. In view of the extreme simplicity of our assumptions about the analytical model, the evident agreement between dotted and solid curves is striking.

On the right of the main peak in Fig. 4(c) there is a small secondary peak in the "experimental" data. This is not related to the peak splitting of Fig. 4(b) or to formula (7) but has a second interesting origin. It arises when two-photon absorption is accompanied by core rearrangement (excitation of the core electron into state $n=2$), which shifts the normal photodetachment peak from $\varepsilon=\omega_L-0.06\approx 0.39$ to $\varepsilon=2\omega_L-0.06-E_{21}\approx 0.445$, in agreement with the figure. Rearrangement into core level 3 is also possible, in which case E_{21} must be replaced by E_{31}, giving a photoelectron energy $\varepsilon\approx 0.32$, and this peak is even smaller but still evident in Fig. 4(c). The effects of core rearrangement on photodetachment spectra have been discussed before in Ref. [5].

In addition, we note that *all atomic parameters are determined once and for all by our negative-ion potential V(x)*. That is, the numerical values of E_g, E_1, E_2, $\langle 1|x|2\rangle$, and γ are not adjustable in any way to improve the fit of the curves in Fig. 3.

Using a somewhat stronger field, $\mathcal{E}_0=0.075$ a.u., we have also studied the time-dependent effects associated with the peak splitting shown in Figs. 3 and 4. These temporal effects are shown in Fig. 6. Again in agreement with our simple analytical model, our exact wave functions show strong Rabi oscillations of the $n=1$ and $n=2$

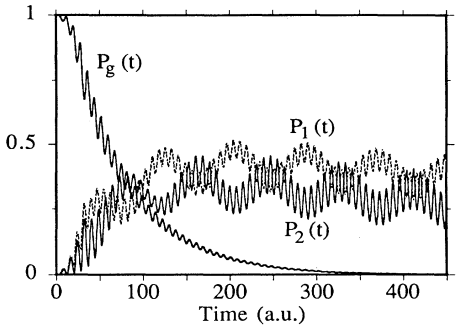

FIG. 6. Time dependence of the ground-state probability $P_g(t)=|\langle g|\Psi(x_1,x_2,t)\rangle|^2$, and the probabilities $P_1(t)$ and $P_2(t)$ to find at least one electron in the lowest two hydrogenic states $\Psi_1(x)$ and $\Psi_2(x)$ and none of the electrons is in the H^- ground state. (const intensity laser pulse with a two-cycle linear turn-on, $\mathcal{E}_0=0.075$ a.u., $\omega_L=0.4$ a.u., the Rabi period $2\pi/\Omega\approx 80$ a.u. corresponds to ≈ 5 optical cycles).

core state probabilities $P_1(t)$ and $P_2(t)$ and it is easy to check that the observed period of these Rabi oscillations is consistent with the numerical Rabi frequency: $2\pi/\Omega\approx 80$ a.u. for $\omega_L=0.4$ a.u. and $\mathcal{E}_0=0.075$ a.u. However, in contrast to the one-electron case [2], we find no Rabi oscillations in the decay of the negative-ion ground state $P_g(t)$ under the condition of exact core resonance. The only oscillations present in the ground-state decay curve occur at twice the laser frequency and can be associated with counter-rotating terms.

In summary, our time-dependent two-electron wave functions predict the existence of a two-electron coherence effect. This effect has a number of unexpected features. There is peak splitting in the photodetachment spectrum of the outer electron, which has no corresponding bound-bound resonance. A dressed-state analysis shows that the *higher-energy* photopeak comes from the *lower-energy* dressed core state. There is ground-state decay without resonant Rabi oscillations. The outer electron's novel properties arise from a core-electron resonance. In particular, the Rabi frequency of the core resonance agrees with the outer electron's photopeak splitting.

These calculations show induced core-electron coherence in the presence of an outer electron, i.e., core coherence that imprints itself on outer-electron dynamics. There appear to be no existing experimental reports of the effect, but on the basis of elementary similarities between the structure of our artificial atom and that of alkali-metal negative ions generally we suggest that a direct laboratory observation of this core-electron coherence might be carried out with Na^-. The principal effects present in a real experiment but not included in our numerical experiments would be the longer laser pulse (by about 10–100 times), the D-line hyperfine structure, and spontaneous emission. Both of the latter two effects become insignificant at moderate laser power. The increased pulse length would simply amplify greatly the core ionization signal and bring the Knight doublet [2] into clear view. The Na^- core resonance (sodium D_1 or D_2 line) has an oscillator strength greater than unity, so

dye laser intensity in the 10^{10} W/cm^2 range should be more than sufficient to split the predicted strong doublet by 30 meV, which is comparable to resolution currently reported for ATI photoelectron studies [9]. We mention Na^- only for illustration. We believe that our model's assumptions and the predictions of formula (7) are sufficiently general to be applicable to many real two-electron systems, atoms as well as negative ions.

This research was supported by the National Science Foundation through Grant No. PHY 92-00542 and PHY 89-20108. R. G. acknowledges partial support through the Feodor Lynen Progam of the A. von Humboldt Foundation of Germany and through the National Science Foundation. We also acknowledge assistance with computing resources from the Pittsburgh Supercomputing Center and the Allied-Signal Foundation.

[1] S. L. Autler and C. H. Townes, Phys. Rev. **100**, 703 (1955). See also P. L. Knight and P. W. Milonni, Phys. Rep. **66**, 21 (1980); P. L. Knight, M. A. Lauder, and B. J. Dalton, *ibid.* **190**, 1 (1990).

[2] P. L. Knight, Opt. Commun. **22**, 172 (1977); J. Phys. B **11**, L511 (1978). For a related experimental report, see Ref. [3].

[3] S. E. Moody and M. Lambropoulos, Phys. Rev. A **15**, 1497 (1977).

[4] M. S. Pindzola, D. C. Griffin, and C. Bottcher, Phys. Rev. Lett. **66**, 2305 (1991).

[5] R. Grobe and J. H. Eberly, Phys. Rev. Lett. **68**, 2905 (1992).

[6] Properties of the soft-core Coulombic potential $V(x)$ are summarized in Q. Su and J. H. Eberly, Phys. Rev. A **44**, 5997 (1991). Applications to one-electron systems have been described in, for example, J. Javanainen, J. H. Eberly, and Q. Su, Phys. Rev. A **38**, 3430 (1988); Q. Su, J. H. Eberly, and J. Javanainen, Phys. Rev. Lett. **64**, 862 (1990); V. C. Reed, P. L. Knight, and K. Burnett, *ibid.* **67**, 1415 (1991). For previous two-electron applications see Refs. [4] and [5].

[7] The space coordinates have been discretized to a 1024×1024 lattice and the time-dependent Schrödinger equation has been solved with a split-operator fast Fourier transform method that has been discussed in detail in M. D. Feit, J. A. Fleck, Jr. and A. Steiger, J. Comput. Phys. **47**, 412 (1982).

[8] The multipeak structure in the lower-energy "normal" doublet arises because the interaction is pulsed rather than steady. This effect was predicted for autoionization by K. Rzazewski, Phys. Rev. A **28**, 2565 (1983) and for resonant multiphoton ionization by D. Rogus and M. Lewenstein, J. Phys. B **19**, 3051 (1986).

[9] P. H. Bucksbaum and T. J. McIlrath (private communication).